

# Numerical Analysis on Current and Optical Confinement of III-Nitride Vertical-Cavity Surface-Emitting Lasers

Ying-Yu Lai<sup>a</sup>, Tien-Chang Lu<sup>\*a</sup>, Tsung-Lin Ho, Shen-Che Huang, and Shing-Chung Wang<sup>a</sup>  
<sup>a</sup>Department of Photonics, National Chiao Tung University, Hsinchu 300, Taiwan

## ABSTRACT

We report on the numerical analysis of the electrical and optical properties of current-injected III-N based vertical-cavity surface-emitting lasers (VCSELs) with three types of current confinement schemes: the conventional planar-Indium Tin Oxide (ITO) type, the AlN-buried type without ITO, and the hybrid type. The proposed hybrid structure, which combines an ITO layer and an intracavity AlN aperture, exhibits not only a uniform current distribution but also an enhanced lateral optical confinement. Thus, the hybrid type design shows a remarkably better performance including lower threshold current and series resistance compared with the planar-ITO type and the AlN-buried type. Furthermore, the multi-transverse mode lasing behavior induced by strong index guiding of the AlN aperture is suppressed to single transverse mode operation by reducing the aperture size. Such design provides a powerful solution for the high performance III-N based VCSELs and is also viable by using current state of the art processing techniques.

**Keywords:** III-nitride, VCSELs, ITO, Buried AlN current apertures, current crowding, lateral index guiding

## 1. INTRODUCTION

Over the past few decades, developments of III-nitride semiconductors are rapidly increased due to their promising potential for practical light emitting diodes and laser diodes [1]-[3]. Among this aspect, III-N with wide-direct-bandgap characteristics are highly appreciated for providing a full-color emission in the visible region, which is very important for many applications, such as lighting, optical storage, projectors, bio-sensing and so on [4]. So far, III-N based edge emitting lasers (EELs) have been realized and become commercialized for high density optical storage applications. But reports on another type of semiconductor lasers, vertical-cavity surface-emitting lasers (VCSELs), with several superior optical characteristics such as single longitudinal mode emission, low divergence angle, low threshold and two-dimensional array capability compared to the EELs, are still limited in the III-nitride system. To date, the continuous wave (CW) current injection of GaN-based VCSEL with hybrid mirrors and full dielectric mirrors are successfully demonstrated [5]-[9]. The key improvement for these devices to achieve room temperature operation is using a thin intra-cavity planar transparent conducting layer, ITO, to reduce the absorption loss but maintaining the current spreading ability within the current aperture. Despite the room temperature current injected GaN-based VCSELs have been successfully demonstrated in the planar-ITO type VCSEL structure, they still suffer from the non-uniform gain distribution, poor lateral optical confinement and the optical loss induced by the intracavity transparent current spreading layer and dielectric current aperture, resulting in a higher optical loss and threshold gain [10]. For aforementioned concerns, we had investigated a high quality current injection microcavity light emitter by inserting an intra-cavity AlN current aperture and removing the transparent current spreading layer to reduce the optical loss and to introduce a lateral current/optical mode confinement [11]. Although the issue of optical loss was reduced, the AlN-buried structure would come across other electrical problems like the limited gain area, current crowding and severe leakage current over active regions to prevent the lasing action.

In this report, we theoretically analyzed both optical and electrical properties of aforementioned planar-ITO type and AlN-buried type cavity designs and also proposed a hybrid structure consisting of a thin ITO layer and a buried AlN current aperture for achieving a good current spreading ability and an additional lateral confinement of both current and optical modes. A three-dimensional model, which was simplified to a cylindrical symmetry two-dimensional scheme, was employed for numerically simulating the intra-cavity phenomena including the current spreading, gain distributions and the optical mode profiles.

## 2. DEVICE STRUCTURE AND SIMULATION MODELS

### 2.1 Device structure

To systematically analyze the impacts of current confinement/spreading layers in the III-N VCSEL, we have taken into account three types of the VCSEL structures mentioned above. Fig.1 (a) shows the proposed hybrid VCSEL structure with the transparent current spreading layer and the buried AlN current aperture. The structure has a  $7\lambda$  thick cavity sandwiched by a bottom 29-pair AlN/GaN epitaxial distributed Bragg reflector (DBR) and a top 10-pair Ta<sub>2</sub>O<sub>5</sub>/SiO<sub>2</sub> dielectric DBR. The cavity composes of a 900 nm-thick n-GaN layer, a 5-pair of In<sub>0.2</sub>Ga<sub>0.8</sub>N (3 nm)/GaN (8 nm) multiple quantum wells (MQWs), a 20 nm-thick AlGaIn electron blocking layer, a 30 nm-thick AlN current aperture inserted into a 100 nm-thick p-GaN layer, a 40 nm-thick ITO current spreading layer. For comparison, Fig. 1(b) to 1(d) display the enlarged p-side cavity structures of the planar-ITO, AlN-buried, and proposed hybrid type VCSELs, which would be used in the following simulation. It is worth noting that the VCSEL structures shown in Fig. 1(b) and Fig. 1(c) are similar to the previous reported devices [6], [11]. Fig. 1(b) shows the planar-ITO VCSEL structure, for which the emitting aperture is defined by the SiN<sub>x</sub> passivation layer (radius of 5 $\mu$ m). Our group has demonstrated lasing action by using this kind of current injection scheme [5], [6]. For the AlN-buried VCSEL structure, the current aperture is defined by the buried AlN layer with a smaller radius of 3.5 $\mu$ m. Owing to the lack of ITO current spreading layer, a smaller current aperture is needed to achieve the laser action. Such device structure is similar to previously reported microcavity light emitting diodes (LEDs), which did not show lasing characteristics [11]. Fig. 1(d) shows our proposed hybrid type structure, combining the ITO spreading layer and the AlN-buried aperture together.

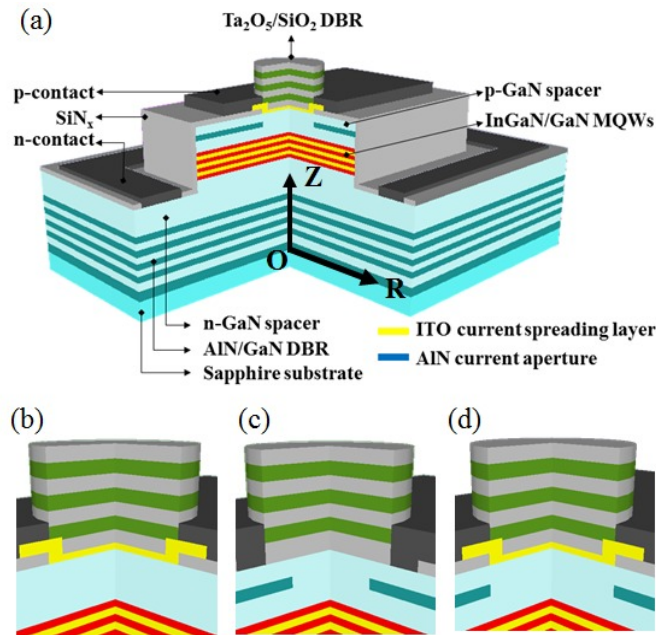


Figure 1. (a) Schematic diagram of proposed ITO-AlN hybrid type GaN-based VCSEL. Z, R, O represent the vertical and lateral coordinate and the original point of simulation model, respectively. Enlarged structures of (b) planar-ITO, (c) AlN-buried, and (d) proposed hybrid type VCSEL.

### 2.2 Simulation model

Since the structure possesses the cylindrical symmetry, the simulation model could be simplified to the two-dimensional (2D) scheme. Coordinates including the vertical direction  $Z$  and the lateral direction  $R$  are based on the original point (O), which lies on the sapphire surface. The commercial software PICS3D [12], which self-consistently comprises the computation of semiconductor transport equations, the optical gain and mode, the quantum well band structure, was employed to model above mentioned VCSEL designs. The carrier transport model includes drift and diffusion of electrons and holes, built-in polarization, Fermi statistics and thermionic emission at hetero-interfaces, as well as spontaneous and defect-related Shockley-Read-Hall (SRH) recombination of carriers were used to determine the carrier transport phenomena. For the calculation of the quantum wells regime, Schrödinger and Poisson equations were solved

iteratively to account for the quantum well deformation with different device bias. Stimulated emission of photons within the quantum well was calculated by a free carrier model including the wurtzite energy band structure. For the optical model, transfer matrix method was used to compute optical transmission and corresponding longitudinal modes between multi-layer gain medium and DBR stacks. For the spatial confined structures, a convenient effective index method (EIM) was employed to describe the transverse modes [13]. Besides, all of simulations are based on the coordinate system shown in Fig. 1(a).

### 3. SIMULATION RESULTS AND DISCUSSION

#### 3.1 Current flow and gain distribution

Since the simulation model is based on the 2D structure, the current flow should be divided into two directions: vertical ( $Z$ ) and lateral ( $R$ ). Fig. 2(a) to 2(c) and Fig. 2(d) to 2(f) depict the vertical-flow and lateral-flow current density distributions in the MQWs around the aperture edges for the planar-ITO, AlN-buried, and hybrid type structures respectively. Fig. 2(a) and 2(d) depict a commonly seen current crowding issue in the planar-ITO case for those current densities flow along the vertical and lateral directions are accumulated at the edge of the apertures. However, for the AlN-buried type, a more serious current crowding problem is observed in Fig. 2(b) and 2(e) due to the lack of current spreading layer and poor hole mobility of the p-GaN layer. The serious current crowding phenomena will induce the thermal accumulation and leakage current problems to limit the device performance. In our proposed hybrid type structure, the ITO layer and AlN current aperture maintain both the good current spreading and the current confinement capability, as shown in Fig. 2(c) and 2(f). The current densities are well confined inside the AlN aperture and are distributed more uniformly in the ITP-capping region compared to the AlN buried type structure without the ITO layer.

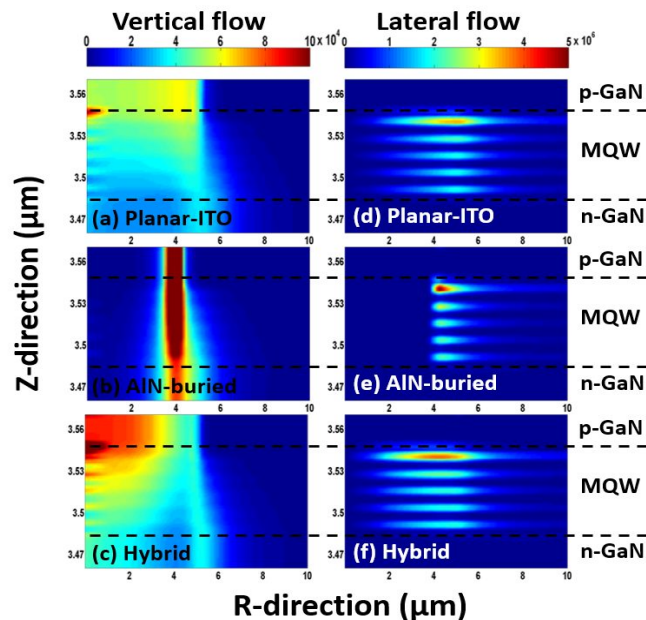


Figure 2. Left column (a) to (c) and right column (d) to (f) represent the vertical-flow and lateral-flow current density in the multiple quantum wells near the aperture edges of the planar-ITO, AlN-buried, and proposed hybrid type VCSEL, respectively. The figure coordinates axes are based on Fig. 1(a).

Figs. 3 show the gain profiles of three types of VCSEL structures. In the planar-ITO structure, the aperture edge region has a higher gain compared to the central region due to the current crowding issue, as shown in Fig. 3(a). The maximum gain disperses along the radial direction from the center of cavity would results in a poor spatial overlapping with the fundamental transverse cavity mode and a higher threshold. For the AlN-buried structure, a serious current crowding problem induced by the lack of the ITO current spreading layer results in a tiny gain area of the gain profile at the edge of the aperture and large optical loss in the center region of cavity, as shown in Fig. 3(b). Therefore, the poor overlapping between gain and fundamental optical mode and high loss in the central region could be the main reason preventing such device far away from lasing in the previous report [11]. As a consequence, we introduce the ITO

spreading layer and buried AlN aperture in the proposed hybrid type structure for maintaining good current spreading and confinement capability. The larger contact area will enhance current injection ability and mitigate the current crowding problem. So we can get a more uniform and broaden gain profile, as shown in Fig. 3(c). Such result would definitely provide a much better performance such as lower threshold current density and possibility of achieving single transverse mode operation.

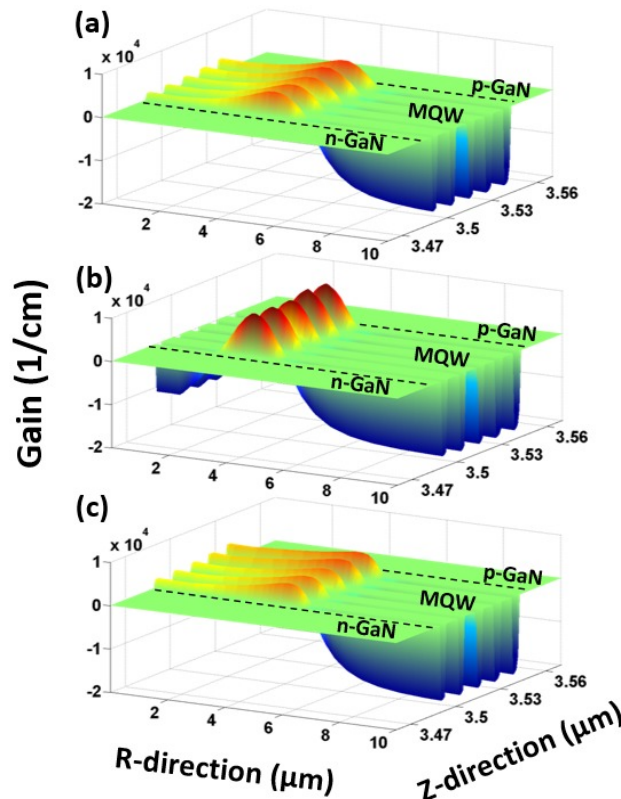


Figure 3. Gain profiles in the multiple quantum wells near the aperture edges. (a) Planar-ITO (aperture radius  $5\mu\text{m}$ ): Slightly aggregation near aperture side, (b) AlN-buried (aperture radius  $3.5\mu\text{m}$ ): Gain gathers together in tiny area. (c) Proposed hybrid type (aperture radius  $5\mu\text{m}$ ): Uniform and broaden gain. The coordinates axis based on Fig. 1. The vertical axes represent the magnitude of gain (1/cm).

### 3.2 Optical mode guiding and gain-optical mode overlapping

In addition to the electronic gain profile, another important role to affect the laser action is the overlapping percentage between the optical gain and cavity mode profile. In the vertical (longitudinal) direction (Z-direction), optical confinements achieved by highly reflective DBRs are almost the same in aforementioned three structures. Thus, the major factor to affect the threshold condition among these three structures would be the lateral (transverse) optical confinement (R-direction). It's noteworthy that AlN-buried type will not be discussed in the following since its laser action is limited by the edge accumulated gain distribution and high absorption loss at the central region from simulation results. In most of the simulation cases, the lasing threshold for the AlN-buried type device is significantly higher than other structure designs and would not be taken into analysis.

In the planar-ITO structure, the ITO layer was set at the node position of the optical field for reducing the absorption loss. But such approach results in negligible index difference and poor lateral optical confinement. As a result, planar-ITO case shows almost no optical guiding effect among different aperture sizes. For the case with a smaller aperture size, although the gain distribution is more central-accumulated, the total overlapping between the optical gain and optical mode is decreased along the lateral direction and results in a higher threshold current (shown in Fig. 4).

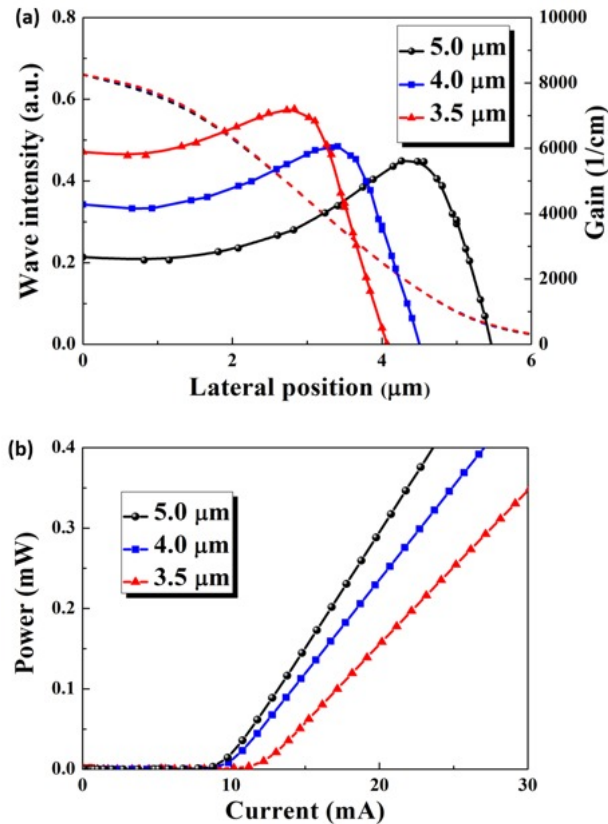


Figure 4. (a) Gain (solid line) and optical mode (dash line) distributions within the quantum wells along the lateral direction. Small aperture size makes the gain profile narrower and centralized but not the optical mode owing to the lack of lateral optical confinement. (b) L-I curves of devices with different aperture size. Threshold current is raised with the small aperture size due to the poor overlapping between the gain and optical mode.

In order to solve the poor index guiding problem in the planar-ITO case, a low index AlN aperture was inserted in the *p*-GaN to provide effective index contrast for transverse optical mode guiding and a high resistance blocking layer for current confinement in the hybrid case. Such scheme could be regarded as a simple step-index circular waveguide and the ITO layer can still be kept. The transverse mode guiding ability could be verified using a normal EIM [13]. The effective index difference ( $\Delta n_{\text{eff}} = n_{\text{eff,cladding}} - n_{\text{eff,core}}$ ) between *p*-GaN core region and AlN cladding can be easily calculated from the local resonance wavelength ( $\Delta\lambda_0$ ) shift shown in the following equation:

$$\frac{\Delta n_{\text{eff}}}{n_{\text{eff}}} \approx \frac{\Delta\lambda_0}{\lambda_0} \quad (1)$$

Thanks to the buried AlN aperture, the hybrid type structure has a better transverse confinement compared to the planar-ITO device with the same radius. The full width at half maximum (FWHM) of 0<sup>th</sup> order mode distribution in the lateral direction is narrowed from 3.5μm in the planar-ITO case to 3μm in the hybrid case. In such a better optical confinement scheme, higher order modes may be evoked for the gain competition. To achieve single mode operation, the AlN aperture size should be reduced to enhance the overlapping between gain region and the 0<sup>th</sup> order fundamental mode. Fig. 5(a) shows spatial distributions of the gain region, 0<sup>th</sup> and 1<sup>st</sup> order modes with different aperture size. From simulation results, device with a smaller aperture radius has a lower threshold of 0<sup>th</sup> mode lasing and higher threshold of 1<sup>th</sup> mode lasing due to the smaller gain-optical mode overlapping for higher order mode (1<sup>th</sup>) and larger mode overlapping for fundamental mode (0<sup>th</sup>), as shown in Fig. 5(b). Thus, the device with a smaller AlN aperture size suggests a wider single-transverse-mode operation range with the injection current and is a very suitable design for high performance GaN VCSELs. We then further optimize the aperture size for lower-threshold single-transverse-mode operation and find that optimum aperture size for the proposed hybrid type VCSEL is 4.5μm, as shown in Fig. 5(c). The



reason of increasing the threshold current at smaller aperture is due to the gain-optical mode overlapping starts to reduce as the aperture radius is smaller than  $4.5\mu\text{m}$  as well as the higher leakage carriers over the MQW when the current density is getting higher.

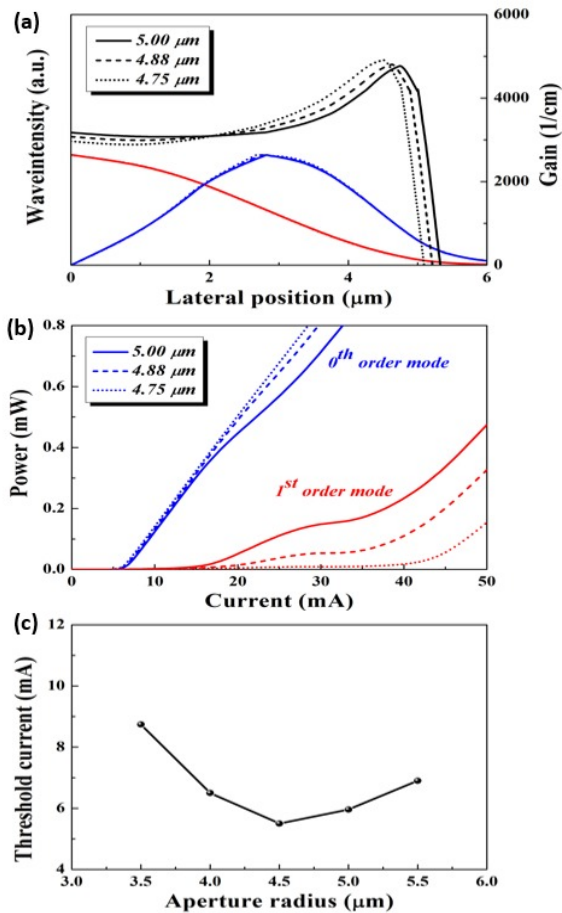


Figure 5. (a) Gain (black lines), 0th (red lines) and 1st (blue lines) order optical mode intensity distributions of different aperture sizes within the quantum wells along the lateral direction. Overlapping of the higher order mode with gain is worsening when the aperture size is narrower. (b) L-I curves of 0th (red lines) and 1st (blue lines) mode lasing among different aperture sizes. (c) Threshold current of hybrid type VCSEL versus different aperture sizes.

### 3.3 C. Output Power Performance and Voltage Characteristics

Fig. 6 shows the light output power-current-voltage (L-I-V) curves of the planar-ITO, AlN-buried and proposed hybrid type VCSEL. Due to the lack of the current spreading layer, the AlN-buried type device has the highest threshold among these three type structures due to the serious problem about current crowding, which may induce additional thermal and leakage effect. For the planar-ITO case, the absence of lateral optical confinement and injection difficulty of the small contact area defined by the  $\text{SiN}_x$  aperture will limit the device performance including threshold current and turn-on voltage. With aforementioned consideration, the proposed hybrid type structure combines the advantages of better current spreading capability of the ITO layer and optical confinement of the buried AlN aperture. Besides, the larger contact area between ITO layer and  $p$ -GaIn attributed to better current spreading and injection capability. According to these advantages, the hybrid type has the best performance. The threshold current could be reduced to even half of that of the planar-ITO type.

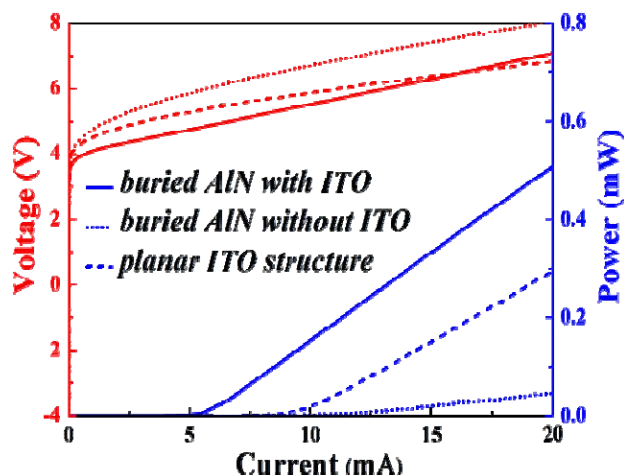


Figure 6. The simulated results of light output power (blue line) and contact voltage (red line) characteristics of hybrid type (dash line) and conventional type (solid line) VCSELs.

#### 4. CONCLUSION

In summary, we have systematically analyzed the electrical and optical characteristics of three types of current and optical confined structures to identify a better design for GaN-based VCSELs. The planar-ITO VCSEL suffers from lack of lateral optical confinement and small contact area for current injection. The AlN-buried VCSEL exhibits a serious current crowding effect and longer current path which results in poor device performance. Our proposed hybrid type VCSEL not only provides better optical confinement but also retains good current injection. These advantages promise a better device design including lowest threshold current and turn-on voltage than previously reported structures. Such hybrid design could be used to realize high performance GaN-based VCSELs and even electrically driven polariton lasers for future scientific investigation.

#### ACKNOWLEDGMENTS

The authors would like to gratefully acknowledge Prof. H. C. Kuo at National Chiao Tung University for technical support. This work has been supported in part by the MOE ATU program and in part by the National Science Council of Taiwan under Contracts NSC100-2628-E-009-013-MY3, and NSC102-2221-E-009-156-MY3.

#### REFERENCES

- [1] Nakamura, S., Senoh, M., Nagahama, S., Iwasa, N., Yamada, T., Matsushita, T., Sugimoto, Y., and Kiyoku, H., "Room-temperature continuous-wave operation of InGaN multi-quantum-well-structure laser diodes with a long lifetime," *Appl. Phys. Lett.* 70, 868-870 (1997).
- [2] Nakamura, S., "The Roles of Structural Imperfections in InGaN-Based Blue Light-Emitting Diodes and Laser Diodes," *Science* 281, 956-961, (1998).
- [3] Nakamura, S., Senoh, M., Nagahama, S., Iwasa, N., Yamada, T., Matsushita, T., Sugimoto, Y., and Kiyoku, H., "Room-temperature continuous-wave operation of InGaN multi-quantum-well-structure laser diodes," *Appl. Phys. Lett.* 69, 4056-4058 (1996).
- [4] Bergh, A. A., "Blue laser diode (LD) and light emitting diode (LED) applications," *Phys. Status Solidi A* 201, 2740-2754 (2004).
- [5] Lu, T. C., Kao, C. C., Kuo, H. C., Huang, G. S., and Wang, S. C., "CW lasing of current injection blue GaN-based vertical cavity surface emitting laser," *Appl. Phys. Lett.* 92, 141102 (2008).
- [6] Lu, T. C., Chen, S. W., Wu, T. T., Tu, P. M., Chen, C. K., Chen, C. H., Li, Z. Y., Kuo, H. C., and Wang, S. C., "Continuous wave operation of current injected GaN vertical cavity surface emitting lasers at room temperature," *Appl. Phys. Lett.* 97, 071114 (2010).

- [7] Higuchi, Y., Omae, K., Matsumura, H., and Mukai, T., "Room-Temperature CW Lasing of a GaN-Based Vertical-Cavity Surface-Emitting Laser by Current Injection," *Appl. Phys. Express* 1, 121102 (2008).
- [8] Omae, K., Higuchi, Y., Nakagawa, K., Matsumura, H., and Mukai, T., "Improvement in Lasing Characteristics of GaN-based Vertical-Cavity Surface-Emitting Lasers Fabricated Using a GaN Substrate," *Appl. Phys. Express* 2, 052101 (2009).
- [9] Onishi, T., Imafuji, O., Nagamatsu, K., Kawaguchi, M., Yamanaka, K., and Takigawa, S., "Continuous Wave Operation of GaN Vertical Cavity Surface Emitting Lasers at Room Temperature," *IEEE J. Quantum Electron.* 48, 1107-1112 (2012).
- [10] Hashemi, E., Gustavsson, J., Bengtsson, J., Stattin, M., Cosendey, G., Grandjean, N., and Haglund, Å., "Engineering the Lateral Optical Guiding in Gallium Nitride-Based Vertical-Cavity Surface-Emitting Laser Cavities to Reach the Lowest Threshold Gain," *Jpn. J. Appl. Phys.* 52, 08JG04 (2013).
- [11] Cheng, B. S., Wu, Y. L., Lu, T. C., Chiu, C. H., Chen, C. H., Tu, P. M., Kuo, H. C., Wang, S. C., and Chang, C. Y., "High Q microcavity light emitting diodes with buried AlN current apertures," *Appl. Phys. Lett.* 99, 041101 (2011).
- [12] PICS3D (Photonic Integrated Circuit Simulator in 3D) by Crosslight Software, Inc., Burnaby, Canada, 2005.
- [13] Ronald Hadley, G., "Effective index model for vertical-cavity surface-emitting lasers," *Opt. Lett.* 20, 1483 (1995).